Subsurface Defect Characterization in Pulsed Phase Thermography by Means of Wavelet Analysis

Gerald ZAUNER, Guenther MAYR, Guenther HENDORFER
Upper Austria Univ. of Applied Sciences, F&E GmbH – Research Center Wels,
Stelzhamerstr. 23, 4600 Wels/AUSTRIA;
gerald.zauner@fh-wels.at

Abstract. Active thermography, in particular Pulse Thermography (PT), is a non-destructive testing method for subsurface defect detection and material characterization. The measurement principle is based on the analysis of an externally generated heat flow which is distorted by flaws or voids. Pulsed Phase Thermography (PPT) was introduced as a signal processing technique for the analysis of pulse thermography time series. The drawback of the Fourier-based approach is the loss of temporal information making quantitative inversion procedures tricky (e.g. defect depth measurements). The Wavelet transform (with Complex Morlet-Wavelets, providing phase and amplitude information) can be used with PT data in a similar way as the Fourier transform but with the advantage of preserving time information. In this paper we review the methodology of PT and the associated signal analysis (Fourier analysis, wavelet analysis) to obtain quantitative defect depth information. We present results of thermal FEM simulations and experimental data and show the advantages of wavelet based signal analysis for defect depth measurements and material characterization.

1. Introduction

When energy is focused onto the surface of an opaque solid material, the material will absorb some of the incident energy. This will produce a localized heat flow in the specimen. Time-dependent heat flow is governed by the one-dimensional heat diffusion equation

$$\frac{\partial^2 T(x,t)}{\partial x^2} = \frac{1}{\alpha} \cdot \frac{\partial T(x,t)}{\partial t} \tag{1}$$

where T is the temperature and α the thermal diffusivity $\alpha = k / (\rho . c)$, ρ, c and k are the mass density, specific heat and thermal conductivity of the medium, respectively. If this energy source is modulated, a periodic heat flow is produced in the material. This resulting periodic heat flow in the material is a diffusive process that produces a periodic temperature distribution called a thermal wave. Three main types of (optical) active thermography techniques are commonly used: Lock-in Thermography (LT), Pulse Thermography (PT) and Pulsed Phase Thermography (PPT). In Lock-in thermography (LT) low frequency sinusoidal heat waves are injected continuously into the specimen. By observing incident and reflected waves with an infrared camera over a period of time, subsurface voids can be found by analyzing the amplitude damping and the phase shift. Usually a lock-in amplifier is used in conjunction to determine the thermal contrast. The probing depth is determined

by the frequency of the sinusoidal excitation, i.e. high modulation frequencies are more suitable for near surface detection and vice versa [1][2].

2. Pulse Thermography analysis based on Fourier-Analysis

In this paper we focus on Pulse Thermography (PT) where a pulse of heat energy is applied to the target specimen, launching a thermal front which propagates into the specimen by thermal diffusion. If there is a subsurface defect, the diffusion rate will be reduced at that specific point and the temperature at this point will be higher due to heat accumulation. The relationship between thermal propagation time t and depth z of the subsurface defect is given by:

$$t \propto \frac{z^2}{\alpha} \tag{2}$$

The pulse duration is varied depending on the thickness of material and its thermal properties (i.e. thermal conductivity). Pulse thermography is a fast method as its inspection only depends on the thermal stimulation pulse. For high thermal conductivity materials, the pulse duration is a matter of milliseconds whereas for low thermal conductivity materials, the required pulse duration is longer: a matter of a few seconds. Serious drawbacks with this technique are reflections of the heat source or the camera, emissivity variations of the sample surface or non-uniformity of heating [1]. The experimental setup for measurements in reflection mode is shown in Fig.1.

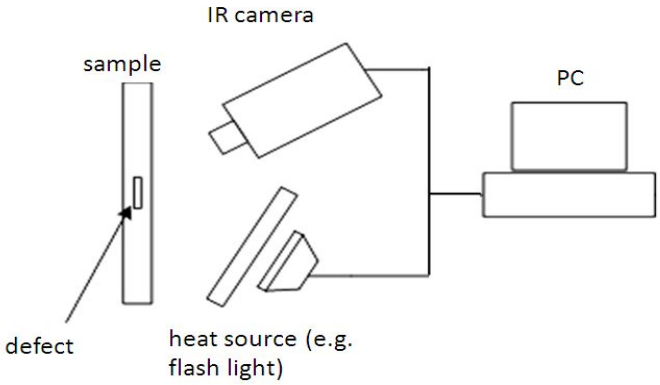

Fig. 1. Experimental setup in Pulse Thermography.

The PPT approach is a combination of the two techniques described above. The Pulsed Phase Thermography technique also uses heat pulses for sample excitation but the analysis is done in the frequency domain. In Lock-In Thermography, a single frequency is tested in the quasi steady-state regime whereas in PPT, all frequencies are tested simultaneously in the transient regime by means of Discrete Fourier Transform (DFT) to derive a phase image:

$$F_n = \sum_{k=0}^{N-1} T(k) e^{2\pi jkn/N} = \mathrm{Re}_n + j\,\mathrm{Im}_n \tag{3}$$

where the subscript n is the frequency increment, N the number of acquired images and T(k) is the kth thermogram. Amplitude and phase information is given by:

$$A_n = \sqrt{\mathrm{Re}_n^{\,2} + \mathrm{Im}_n^{\,2}}\,, \quad \phi_n = \tan^{-1}\left(\frac{\mathrm{Im}_n}{\mathrm{Re}_n}\right) \tag{4}$$

For a predetermined sampling rate ($fs=1/\Delta t$), the total number of images N dictates the minimum available frequency ($fmin=fs/N$). The maximum available frequency is given by half the sampling rate ($fmax= fs/2$), since $n_{max}=N/2$, *i.e.* the Nyquist frequency fc. To go deeper below the surface, large Δt and/or large N must be used. Hence, the sampling and truncation parameters can be optimized for every inspected depth [4]. The choice of the thermal pulse duration also affects the results. The longer the pulse in the time domain, the more high frequency components are suppressed and the energy is concentrated in the low frequencies. If defects very near the surface are observed a much shorter heat pulse must be used to keep the high frequency signal components (which however implies the practical problem of depositing enough energy in a very short time to cause a measurable temperature contrast).

The PPT technique takes shorter measurement time and offers deeper probing depth under the surface and has better defect shape resolution compared to the thermal contrast method of PT. The drawback of the Fourier-based approach however is the loss of temporal information making quantitative inversion procedures tricky (i.e. quantitative defect depth measurements). This is related to the fact, that Fourier transforms decompose a signal into infinite, circular functions [1][3][4].

3. Wavelet Analysis

1.1 Continuous Wavelet Transform

The Wavelet Transform (WT) was introduced as an alternative approach to time/frequency analysis to overcome problems with the frequency resolution in standard STFT (Short Term Fourier Transform). Instead of using periodic functions in the transformation kernel, it uses a waveform function, the so-called wavelet function. While STFT provides uniform time resolution for all frequencies, WT provides high time resolution and low frequency resolution for high frequencies and high frequency resolution and low time resolution for low frequencies. This is obtained by scaling and translating a basis function, which is called the mother wavelet. These functions can be expressed as:

$$\psi_{a,b} = \frac{1}{\sqrt{|a|}}\psi\left(\frac{x-b}{a}\right), \qquad a,b \in \Re \quad a \neq 0 \tag{5}$$

where $\psi(x)$, referred to as the mother wavelet, is a time/space function with finite energy and fast decay, and a and b represent the dilation and translation parameters respectively. The Continuous Wavelet Transform (CWT) is defined as:

$$CWT(a,b) = \int_{-\infty}^{\infty} \psi_{a,b}\, f(x)\, dx \tag{6}$$

Hence, with the CWT a signal is decomposed into its frequency components by scaled wavelet functions.

1.2 Complex Morlet Wavelet

The complex Morlet Wavelet is defined by:

$$\psi(x) = \sqrt{f_b \pi}\, e^{i 2\pi f_c x}\, e^{-\frac{x^2}{f_b}} \tag{7}$$

f_c … wavelet center frequency, f_b … bandwidth parameter

The Morlet Wavelet is a complex sinusoid within a Gaussian envelope, where the central frequency f_c determines the number of significant oscillations of the complex sinusoid within the Gaussian window. The sinusoidal characteristic and the linear phase property (Fig.2) make the complex Morlet Wavelet an ideal candidate for PT analysis.

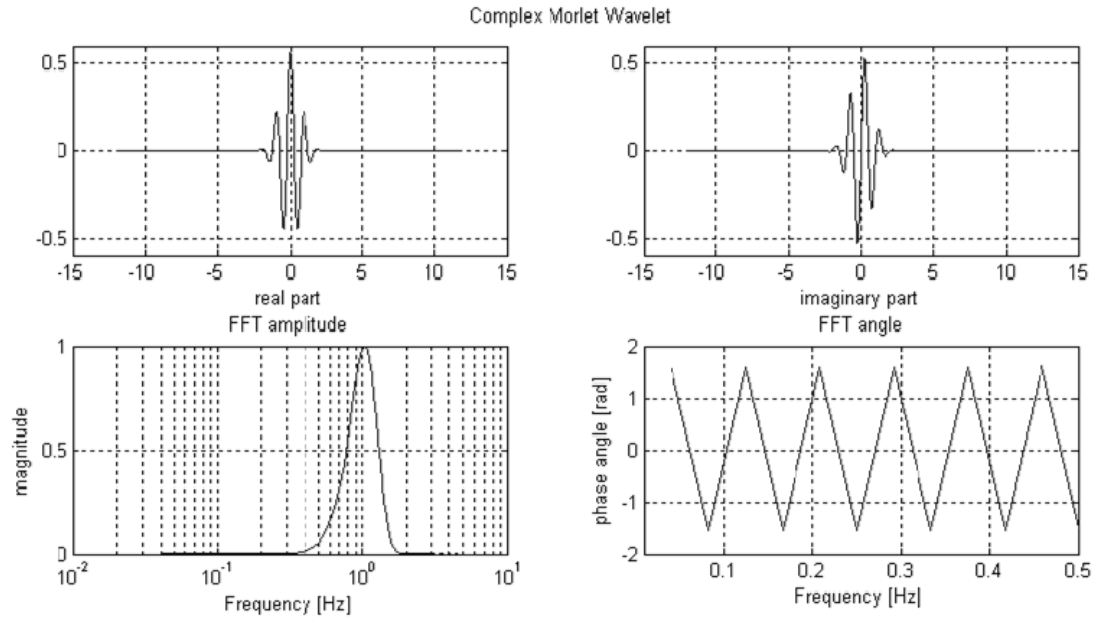

Fig.2: Complex Morlet wavelet (f_b = 1 Hz, f_c = 1 Hz, sampling period Δt = 1s) and corresponding power and phase spectrum

As the mother wavelet can be scaled, a very fine 'tuning' of the frequency (or better, 'pseudo'-frequency) is possible. The relation between the wavelet scale *a* and a 'pseudo'-frequency f_a can be established by the following formula :

$$f_a = \frac{f_c}{a \cdot \Delta t} \tag{8}$$

with f_a = pseudo-frequency corresponding to the scale [Hz], f_c= wavelet center frequency [Hz], Δt= sampling period.

By choosing the appropriate wavelet frequencies f_b, f_c and scale *a* a band-pass/edge like frequency spectrum can be generated which should match or cover the amplitude spectrum of the expected contrast signals.

4. Pulse Thermography analysis with the Complex Morlet Wavelet

The disadvantage of the Fourier-based method is intrinsic to the Fourier transform which suppresses all temporal information, i.e. direct defect depth information is lost as sub-surface defect depth is proportional to the square root of time. The Complex Wavelet Transform can be used with PT data in a similar way as the Fourier transform but with the

advantage of preserving time information of the signal, which can then be correlated to defect depth, and in this way allows a quantitative evaluation [5]. In practice, an area of the specimen without any defect is chosen and taken as a signal reference. This reference is subtracted from the other measurement points (Fig.3a). The resulting thermal contrast signal representing the difference of the temporal evolution of the surface temperature at a defective position and the sound/reference position is shown in Fig.3b.

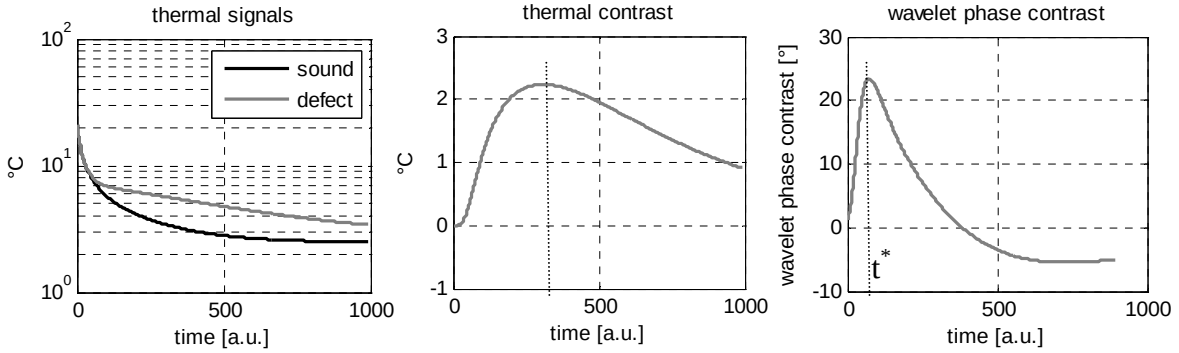

Fig.3a: Sound & defect signal **Fig.3b**: Thermal contrast (defect – sound) **Fig.3c**: Wavelet phase contrast

The resulting wavelet phase contrast signal is shown in Fig.3c. The instant of time t^* when a maximum is reached corresponds to the defect depth. We propose additionally to use the according phase contrast value to derive some supplementary information about the thermal reflection properties at the defect interface. This is motivated by the fact that thermal waves are thought to 'reflect' between media of different thermal characteristics (thermal wave reflection coefficient *R*) [6][7].

5. Simulation results

We used 2D axial symmetric finite element simulations (simulation parameters are listed in Tab.1) to derive the temporal evolution of surface temperatures in isotropic graphite epoxy materials with defects at different depths. The simulation was limited to N =1024 samples with a sampling frequency f_s of 25Hz (i.e. a minimum frequency of 0.024 Hz) which corresponds to the technical specifications of a standard infrared camera. The defect was assumed to be a 'circular' disk of 1cm diameter and 'thickness' of 1mm at different depths ranging from 0.5mm to 3.5mm and consisting of different materials.

Table 1. Simulation parameters

		bulk	**defect**		
		CFK (⊥)	**air**	**Teflon**	**brass**
k	W/(m K)	0.64	0.07	0.23	125
ρ	kg/m^3	1600	1.2	2200	8450
c	J/(kg K)	1200	1005	1040	370

Fig.4 (upper graph) shows the correlation between defect depth and position of the phase maximum. In this regard, the analyzing wavelet was adjusted to show a (quasi-)linear dependency, while the lower graph shows the corresponding phase contrast values at these maxima positions. The material-defect interface is graphite epoxy (⊥) and air with a thermal reflection coefficient of approx. R = 0,98. The wavelet phase contrast considerably decreases in a linear way with increasing depth.

The simulation was repeated, but now with metal (brass) as the defect material leading to a thermal reflection coefficient of R = - 0.89 (remark: the wavelet parameters were kept constant in all experiments). The resultant phase maxima curve and phase contrasts are shown in Fig.4-middle). Again, a linear dependency can be observed but now with increasing phase contrast as the defect depth increases.

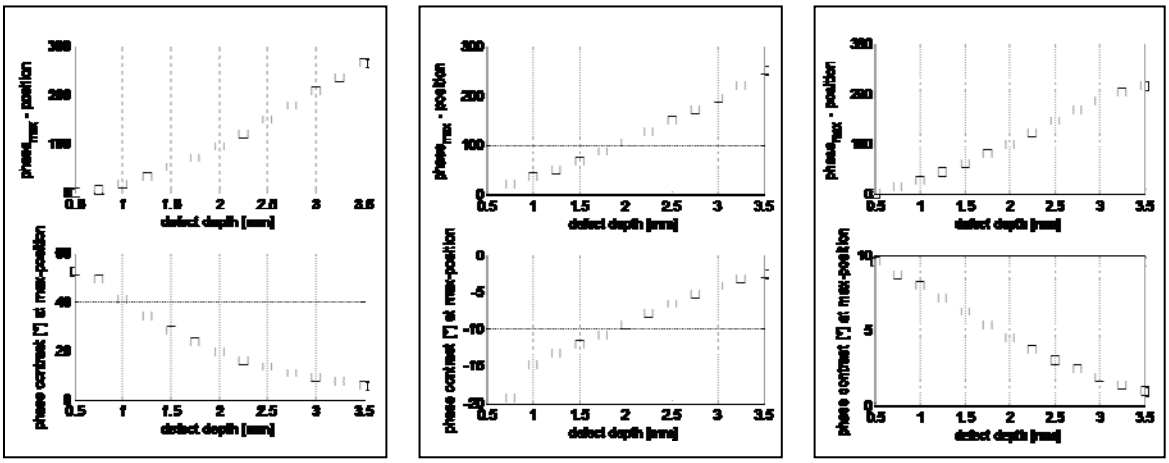

Fig.4: defect depth variation; left: graphite-epoxy/air R=0.98; middle: graphite-epoxy/metal (brass), R = -0.89; right: graphite-epoxy/Teflon R = 0,2.

The third graph (Fig.4-right) shows the results obtained with Teflon as defect-material – the phase contrast decreases with depth, but the relative contrast change is reduced (due to the fact that the reflection coefficient is close to zero and in this way barely influences the thermal wave). In all 3 cases the phase maximum / depth correlation is almost identical. However, the associated phase contrast values show characteristic behavior related to defect depth. Additionally, we simulated the same inclusions but now at a constant depth of 2mm while varying the defect-'thicknesses' (ranging from 0.5mm to 2mm, Fig.5). The derived defect depths were almost constant in all 3 cases (indicated by a constant phase-maximum position of approx. 100, as indicated by Fig.5 upper graphs) while the according phase contrasts showed 'reverted' characteristics compared to the previous results (with deviations from the linear slope characteristic especially in the case of the Teflon defect, supposable caused by the beginning influence of lateral heat flows). These results indicate the possibility of characterizing a defect more precisely by including the phase contrast in the analysis, particularly if high thermal reflection coefficients are expected.

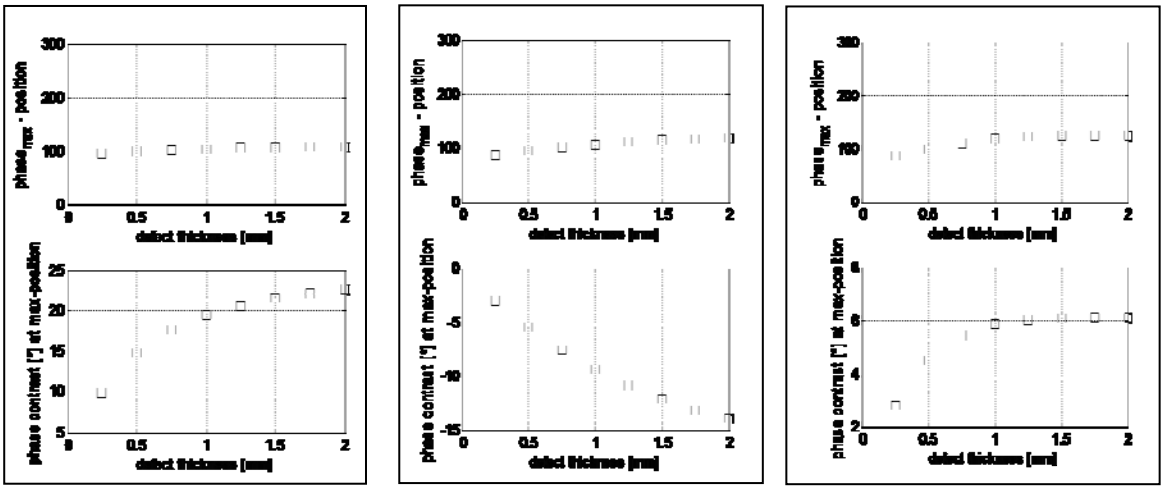

Fig.5: defect thickness variation; left: graphite-epoxy/air R=0.98; middle: graphite-epoxy/metal(brass) R=-0.89; right: graphite-epoxy/Teflon, R = 0.2.

6. Experimental results

Exemplarily, we applied the proposed approach to a real defect in a wood plastic composite (WPC). The defect is characterized by a complex shaped subsurface delamination. The defect geometry was first measured with 3D-computed tomography (3D-CT) to obtain the 'ground truth'. In particular we are interested in defect depth information (i.e. the depth z from the sample surface to the air inclusion). Furthermore, the 'thickness' of the delamination (referred to as 'defect thickness') was determined by 3D-segmentation of the CT results, giving detailed information about the true structure of the sample and the defect. The resolution of the 3D-CT image is approx. 100µm per pixel. Examples of the 3D-CT results are shown in Fig.6 (left: a photograph of the WPC sample, size 80x80x3mm; middle: a cross section image in the x-y-plane approx. 1mm below the surface; right: a cross section image in the x-z-plane showing the complex shape of the delamination). The thermographic measurement system consisted of an un-cooled micro-bolometer camera FLIR PM695 (NETD 80mK, 320x240 pixels) with a frame rate of 25 images/sec, IR-macro-lens (max. resolution 0.2mm/pixel) and a flash light (1500 Ws). Fig.7 shows the results obtained by the proposed method (left) and the corresponding 3D-CT measurement results (right). The upper figures represent defect depth information (white: near the surface; black: deeper below the surface) whereas the lower figures represent the corresponding defect thicknesses (i.e. the thickness of the air inclusion / delamination).

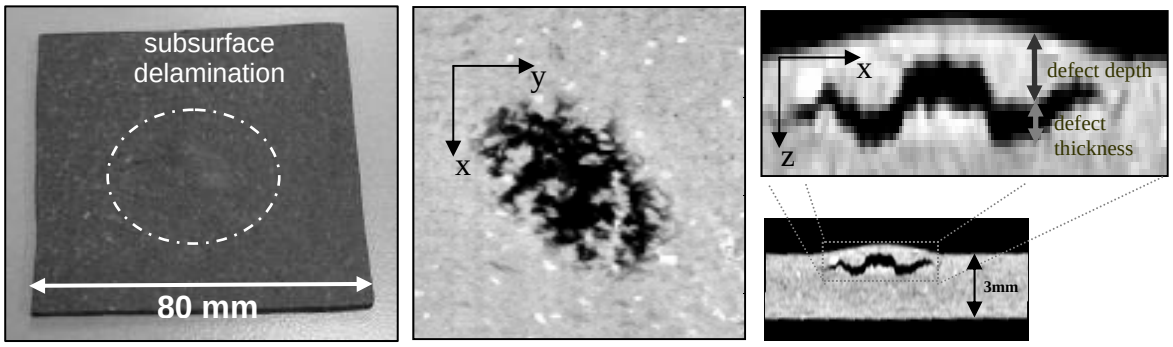

Fig.6: Defect in a wood plastic composite (WPC), characterized by 3D-computed tomography.

7. Summary

In this paper the application of Wavelet analysis based on the complex Morlet Wavelet in the context of Pulse Thermography was presented. In addition to the defect depth analysis (which is based on the determination of the instant of time when a Wavelet phase maximum occurs), we propose to include the according Wavelet phase contrast into the analysis, to obtain supplementary information about the subsurface defect structure – in particular the thermal reflection coefficient. We showed exemplarily, that in Pulse Thermography, the Wavelet based phase contrast is also characteristically influenced by defect depth and defect material (i.e. thermal reflection coefficients.) This was shown on the basis of selected examples of thermal finite element simulations (taking into account different defect geometries, materials and defect depths). We compared in detail the results obtained by Wavelet based Pulsed Phase Thermography for the characterization of a complex 3D shaped subsurface defect with those from 3D computed tomography at a high spatial resolution of approx. 100µm. The results show good correlation and in this way the potential of Wavelet based phase contrast analysis for quantitative defect characterization.

In particular, the ambiguity of classical Fourier based PPT results may be reduced using the proposed approach.

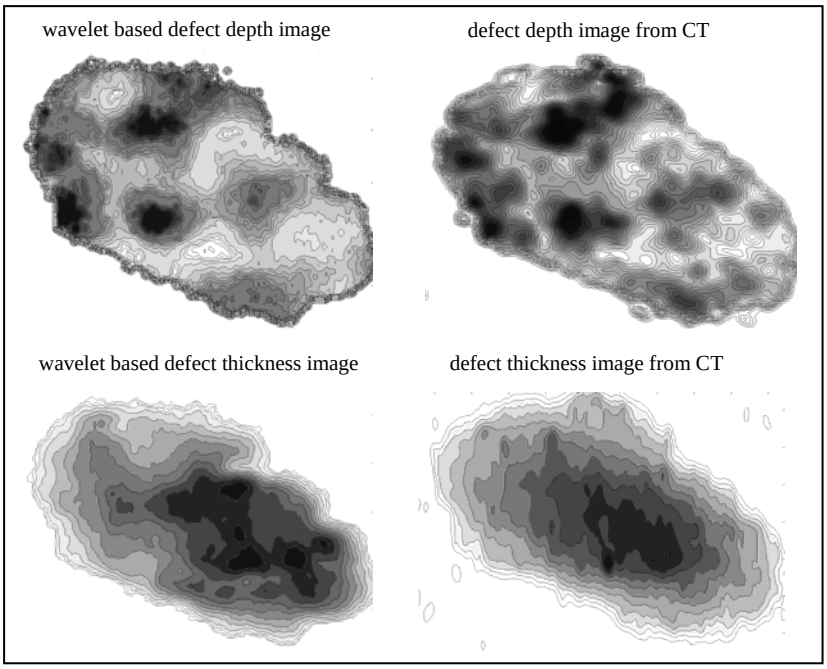

Fig.7: Comparison of results obtained by the proposed method (left) and 3D-computed tomography (right).

References

[1] X. Maldague et al: “Theory and practice of infrared technology for non-destructive testing”, J. Wiley & Sons, 2001.

[2] G. Busse et al: “Thermal wave imaging with phase sensitive modulated thermography”, J. of Applied Physics, vol. **71**/8, 1992

[3] X. Maldague, S. Marinetti: “Pulse Phase Infrared Thermography”, J. Appl. Phys., **79**(5): 2694-2698, 1996.

[4] E. Ibarra-Castanedo C. and X. Maldague: “Defect depth retrieval from pulsed phase thermographic data on Plexiglas and aluminum samples”, Proc. of Thermosense XXVI, Volume 5405, pp. 348-356 (2004).

[5] F. Galmiche, X. Maldague, S. Valler, J.-P. Couturier: “Pulsed phased thermography with the wavelet transform”, AIP Conference Proceedings – Review of Progress in Quantitative Non-destructive Testing, vol. **509**, pp. 609-616

[6] G. Zauner, G. Mayr, G. Hendorfer:” Wavelet based subsurface defect characterization in pulsed phase thermography for non-destructive evaluation”, Proceedings of SPIE-Wavelet Applications Volume 7248, San Jose / USA, 2009

[7] R. Li Voti et al: ”Thermal waves physics”, J. of Optoelectronics and Advanced Materials Vol.3, p 779-816, 2001.